TAMPERE UNIVERSITY OF TECHNOLOGY

Applicability of 3GPP Indoor Hotspot Models to the Industrial Environments

Citation
Wang, W., & Lohan, E-S. (2018). Applicability of 3GPP Indoor Hotspot Models to the Industrial Environments. In *2018 8th International Conference on Localization and GNSS (ICL-GNSS)* [8440902] IEEE. https://doi.org/10.1109/ICL-GNSS.2018.8440902

Year
2018

Version
Peer reviewed version (post-print)

Link to publication
TUTCRIS Portal (http://www.tut.fi/tutcris)

Published in
2018 8th International Conference on Localization and GNSS (ICL-GNSS)

DOI
10.1109/ICL-GNSS.2018.8440902

Copyright
This publication is copyrighted. You may download, display and print it for Your own personal use. Commercial use is prohibited.

Take down policy
If you believe that this document breaches copyright, please contact cris.tau@tuni.fi, and we will remove access to the work immediately and investigate your claim.

Download date:04.03.2021

Applicability of 3GPP Indoor Hotspot Models to the Industrial Environments

Wenbo Wang and Elena Simona Lohan
Tampere University of Technology, Finland
{wenbo.wang, elena-simona.lohan}@tut.fi

***Abstract*—In this paper we study the applicability of the 3GPP Indoor Hotspot model (InH from TR38.901 document) to the indoor industrial environments with moving robots. We will show the impact of carrier frequencies on the expected path losses as we move from cmWave to the mmWave bands, we will present the upper bounds on the capacity expected at different available carrier frequencies and different 3D distances, and we will also discuss the results in the context of receiver sensitivities of various Internet-of-Things solutions for industrial environments, such as Sigfox, LoRa, BLE or Wi-SUN.**

***Index Terms*—3GPP Indoor hotspot channels (InH), open office, mixed office, cmWave, mmWave, industrial environments**

I. Introduction

Industrial environments refer to those scenarios where an industrial activity takes place, such as manufacturing factories, oil and mining fields, chemical plants, etc. The two major targets in an industrial environment are to improve work safety and to increase the production efficiency. Factory automation is one of the top applications envisioned by the researchers in 5G communications areas [1].

In a factory automation environment, the hotspot areas refers to areas with a high density of industrial nodes, such as robots, sensors, human controllers, etc., which need both uplink and downlink connections to the access network. The reliability of such connections should be very high; the researchers usually talk about "ultra-reliable connections" in such scenarios [1], [2] and they measure the reliability for example, in terms of diversity (spatial, time or frequency diversity) or outage probabilities [1], [3].

Traditionally, the wireless connections in industrial environments have been covered by industrial-specific standards such as ISA 101.11a or WirelessHART. In recent years however, more and more focused has shifted towards cellular wireless communications such as 4G (LTE) and 5G (next generation of wireless communications). The research efforts related to 4G and 5G communications are led by 3GPP standardization body, which has already published various channel models to support a wide range of carrier frequency bands, basically anything between 0 GHz and 100 GHz [4].

One of these channel models is the he 3GPP indoor hotspot (InH) path-loss channel model, defined in [4], [5] as an indoor scenario with small cells, a Base Station (BS) or Access Node (AN) mounted below the ceilings and the users (or robots) moving inside the building. The key characteristics of InH, as defined in [4] are high user throughput and indoor coverage. The path-loss and shadowing models characterizing InH environments can be found in [5] and they form the basis of our research work in this paper. The goal is to analyse the receiver performance at different carrier frequencies, ranging from sub-GHz cmWaves to mmWaves, and different bandwidths. Performance metrics such as capacity and outage probabilities are investigated and they are discussed in terms of industrial environment constraints. The received signal strength predicted by the maximum link budgets, according to the 3GPP InH model, will also be compared with several commercial receiver sensitivities of various Internet-of-Things solutions for industrial environments, such as Sigfox, LoRa, BLE or Wi-SUN.

Related work can be found in [6], [7]. For example, modified 3GPP channel models can be found in [6] (LTE indoor topology, dynamic case), but used in a different context (smart home environment) and looking only at fixed carrier frequency (3.5 GHz). Moreover, no comparison with the original 3GPP channel models was provided in [6]. In [7], the authors compare the 3GPP Urban Microcell (UMi) and Urban Macrocell (UMa) with the NYUSIM channel models for 5G wireless communications and draw the conclusion that NYUSIM channel model is more optimistic than the 3GPP ones, as it provides better spectral efficiencies. Our work is complementary to the work in [7], as we focus on a different 3GPP channel, namely the InH channel.

To the best of the Authors' knowledge, there is currently of lack of research papers investigating the InH indoor channel model of 3GPP under concrete case studies, such as industrial environments. Our study here aims to address this gap.

II. 3GPP Indoor Hotspot model (InH)

The 3GPP InH model, as found in [5], defines the path losses via a deterministic part (distance dependent) and a random part (due to shadowing) and under two situations: i) Line of Sight (LOS) and ii) Non Line of Sight (NLOS), by giving also the LOS probability. The path loss, including shadowing, under LOS case PL_{LOS} is given by

$$\begin{aligned} PL_{LOS} &= 32.4 + 17.3\log_{10}(d_{3D}) + 20\log_{10}(f_c) \\ &+ \xi_{LOS} \end{aligned} \quad (1)$$

where d_{3D} is the 3D distance between the access node and the robot (given in meter), f_c is the carrier frequency (given in GHz) and ξ_{LOS} is the shadowing under LOS conditions,

modelled as a Gaussian variable of zero mean and standard deviation $\sigma_{SF_{LOS}}$, and $\sigma_{SF_{LOS}} = 3, 1m \leq d_{3D} \leq 150m$.

Similarly, the path loss, including shadowing, under NLOS case PL_{NLOS} is given by

$$\begin{aligned} PL_{NLOS} &= \max(PL_{LOS}, 38.3\log_{10}(d_{3D}) \\ &+ 17.30 + 24.9\log_{10}(f_c)) + \xi_{NLOS} \end{aligned} \tag{2}$$

where ξ_{NLOS} is the shadowing under NLOS conditions, modelled as a Gaussian variable of zero mean and standard deviation $\sigma_{SF_{NLOS}}$ and $\sigma_{SF_{NLOS}} = 8.03, 1m \leq d_{3D} \leq 150m$.

The LOS probability is defined under two cases:

1) Mixed indoor

$$Pr_{LOS} = \begin{cases} 1, & d_{2D} \leq 1.2m \\ e^{(-\frac{d_{2D}-1.2}{4.7})}, & 1.2m < d_{2D} \leq 6.5m \\ 0.32e^{-\frac{d_{2D}-6.5}{32.6}}, & 6.5m < d_{2D} \end{cases} \tag{3}$$

2) Open indoor

$$Pr_{LOS} = \begin{cases} 1, & d_{2D} \leq 5m \\ e^{(-\frac{d_{2D}-5}{70.8})}, & 5m < d_{2D} \leq 49m \\ 0.54e^{-\frac{d_{2D}-49}{211.7}}, & 49m < d_{2D} \end{cases} \tag{4}$$

Thus, in one d_{2D} interval the path losses plus shadowing PL_{InH} under the 3GPP InH model are given by

$$\begin{aligned} PL_{InH} =& Pr_{LOS}(PL_{LOS} + \xi_{LOS}) \\ &+ (1 - Pr_{LOS})(PL_{NLOS} + \xi_{NLOS}) \end{aligned} \tag{5}$$

III. 3GPP MODEL ANALYSIS

If we only consider the shadowing effect on the calculation of InH path loss, in the context of 3GPP TR38.901 document, we could derive the below form for the expected overall path loss,

$$\begin{aligned} PL = \sum_{n=1}^{N} P(Pr_{LOS}^{(n)}|\cdot)\Big[& Pr_{LOS}^{(n)}(PL_{LOS} + \xi_{LOS}) \\ & + (1 - Pr_{LOS}^{(n)})(PL_{NLOS} + \xi_{NLOS})\Big] \end{aligned} \tag{6}$$

where $P(Pr_{LOS}^{(n)}|\cdot)$ is the $n-th$ posterior given by the $n-th$ d_{2D} segment in either the mixed office or the open office scenario, $Pr_{LOS}^{(n)}$ is Pr_{LOS} in the $n-th$ d_{2D} segment, N is the total number of d_{2D} segments in one scenario.

It is obvious that the overall path loss in eq. (6) follows a Gaussian distribution$PL \sim \mathcal{N}(\mu_{PL}, \sigma_{PL}^2)$. The shadowing ξ_{LOS} and ξ_{NLOS} are modelled as Gaussian variables, the linear summation of Gaussian variables follows a Gaussian distribution. The mean value (μ_{PL}) and variance value (σ_{PL}^2) are given as below,

$$\begin{cases} \mu_{PL} = \sum_{n=1}^{N} P(Pr_{LOS}^{(n)}|\cdot)\Big[Pr_{LOS}^{(n)} PL_{LOS} \\ \qquad + (1 - Pr_{LOS}^{(n)})PL_{NLOS}\Big] \\ \sigma_{PL}^2 = \sum_{n=1}^{N} \Big[P(Pr_{LOS}^{(n)}|\cdot)Pr_{LOS}^{(n)}\sigma_{SF_{LOS}}\Big]^2 \\ \qquad + \Big[P(Pr_{LOS}^{(n)}|\cdot)(1 - Pr_{LOS}^{(n)})\sigma_{SF_{NLOS}}\Big]^2 \end{cases} \tag{7}$$

A. Calculation of the posterior

The posterior in eq. (7) is determined by the segments, the lower and upper bound of d_{2D} and the distribution of robots. In 3GPP TR38.901, the corresponding parameters are given, we select relevant ones and present in Table I.

TABLE I
PARAMETERS OF INDOOR SCENARIOS

Parameters	Indoor open office (mixed office)
Layout	$120m \times 50m \times 3m$
Hotspot antenna height	3m (ceiling)
Robot location height	1m
Min. hotspot-robot distance (d_{2D})	0m
Max. d_{3D} distance	150m
Robot distribution (horizontal)	uniform

We calculate the $\max(d_{2D}) \approx 149.9967(m)$, since in the Table I it mentions that the robot follows the uniform distribution horizontally, thus $d_{2D} \sim \mathcal{U}(0, 149.9967)$, now we could derive the posterior as the below,

$$P(Pr_{LOS}^{(n)}|\cdot) = \int_{d_1}^{d_2} \frac{1}{149.9967} d_{d_{2D}} \tag{8}$$

where d_1 and d_2 are the lower and upper bound of d_{2D} in one segment respectively.

The value of posterior $P(Pr_{LOS}^{(n)}|\cdot)$ is given in the Table .

TABLE II
POSTERIOR $P(Pr_{LOS}^{(n)}|\cdot)$

Posterior	Value
Indoor Mixed office	
$P(d_{2D} \leq 1.2m)$	0.008
$P(1.2m < d_{2D} \leq 6.5m)$	0.035
$P(6.5m < d_{2D})$	0.957
Indoor open office	
$P(d_{2D} \leq 5m)$	0.033
$P(5m < d_{2D} \leq 49m)$	0.293
$P(49m < d_{2D})$	0.674

IV. Industrial environment constraints

The performance criteria regarding the (indoor) industrial environments are typically related to the reliability of the communications links, end-to-end latency, and workers safety. In our simulations, we will focus on several communication-related performance criteria, namely capacity and outage probabilities. These summarize in Table III. An N/A values means that the target criterion was not given in the considered reference.

TABLE III
Industrial (indoor) environment targets and constraints

Reference	Outage probability constraint	SNR targets [dB]	Capacity targets
[3]	$< 10^{-2}$	20	N/A
[8]	$< 10^{-2}$	-20 (LoRa) 7 (Sigfox)	N/A
[9]	N/A	$4.5 - 15$	5 bits/s/Hz
[10]	N/A	20 [1]	18.9 bits/s/Hz
[11]	$= 10^{-9}$	$15 - 20$	N/A

V. Link budget, receiver sensitivity, outage probabilities, and capacity

The received signal power P_R is given by

$$P_R = P_T + G_T - L_T - PL_{InH} + G_R - L_R, \qquad (9)$$

where P_T is the transmit power, G_T and G_R are the antenna gains at the transmitter and receiver sides, respectively, L_T and L_R are the cable losses at the transmitter and receiver sides, respectively, and the path loss PL_{InH} is given by the eq. (5).

Assuming a receiver sensitivity $P_{R_{min}}$, the outage probability p_{out} is defined here as the probability that the received signal strength from eq. (9) is smaller or equal to $P_{R_{min}}$, i.e.

$$p_{out} = proba(PL_{InH} \geq P_T + G_T - L_T + G_R - L_R - P_{R_{min}}) \qquad (10)$$

The PL_{InH} term is a randomly distributed variable, which depends on the shadowing under LOS and NLOS conditions. In addition, the SNR (in dB scale) is related to the received signal power P_R via

$$SNR = P_R + 174 - 10log_{10}(B_W) - N_F \qquad (11)$$

where B_W is the receiver bandwidth in Hz, N_F is the receiver noise figure (in dB), and P_R is given in eq. (9). We remark that some authors define the outage probability as the probability that SNR falls below a certain threshold.

The data capacity or throughput C assuming an efficiency $\eta < 1$ (typically between 0.4 and 0.7 [10]) with respect to the Shannon capacity is given by

$$C = \eta B_W log_2\,(1 + SNR) \qquad (12)$$

with SNR given in eq. (11). Several examples of typical receiver sensitivities $P_{R_{min}}$ for different chipsets and various IoT technologies are shown in Table IV.

[1]It is the reference SNR in the MIMO system.

TABLE IV
Receiver sensitivities in commercial IoT chipsets

Chipset	IoT technology	$P_{R_{min}}$ [dBm]
Semtech SX1257	LoRa	-142
Microchip RN2483	LoRa	-146
BP35A1	Wi-SUN	-103
CC2541	BLE	-90
CC2520	ZigBee	-98
Telit LE51-868 S	Sigfox	-126

VI. Simulation results

This section focuses on path-loss-related results with 3GPP InH models (open and mixed offices) for an LTE-like signal. The main simulation parameters are shown in Table V.

A. Path loss versus 3D distance and carrier frequency

In this simulation scenario, we assume that the coordinate of access node is $(0, 0, 3)$ m and the height of robot is 1m. The horizontal coordinate of robot is randomly generated under the constrain $d_{3D} \leq 150$. The path loss is calculated according to eq. (5), which considers both the LOS and NLOS cases.

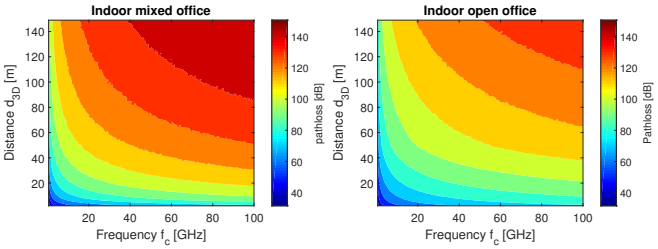

(a) InH Mixed office (b) InH Open office

Fig. 1. The path loss of InH mixed office and open office model. The result is based on 1000 Monte Carlo runs.

Figure 1 shows that at equal carrier frequencies and 3D distances, the indoor mixed office suffers higher path loss compared to the indoor open office. In addition, the value of path loss in indoor mixed office ascends faster than that in indoor open office, along with either the carrier frequency or the 3D distance. The maximum path losses at the considered 3D distances (i.e., maximum 150 m) of the indoor mixed office and the indoor open office are close to 160 dB and 140 dB, respectively.

B. Capacity versus 3D distance and carrier frequency

In this simulation scenario, we use the same settings as the Section VI-A for some assumptions. Other assumptions are given in the Table V.

The discussion of capacity falls into two cases. In the simulation scenario of capacity versus carrier frequency, we choose two 3D distances, namely 6.1347 meters and 50.7163 meters, in order to test the performance of InH indoor model

TABLE V
PARAMETERS OF THE CAPACITY SIMULATION

Parameters	Value	Value
LTE-like signal	**Downlink case**	**Uplink case**
Transmitted power $P_T(P_t)$	43dBm	23dBm
Transmitter antenna gain $G_T(G_t)$	18dBi	0dBi
Transmitter feeder loss $L_T(L_t)$	4dB	0dBi
Receiver antenna gain $G_R(G_r)$	0dBi	18dBi
Receiver feeder loss $L_R(L_r)$	0dB	4dB
Receiver noise figure $N_{FR}(N_{Fr})$	7dB	5dB
Downlink bandwidth B_W	2MHz	1MHz
Efficiency η	0.6	0.6

in the near and far area along with the carrier frequency. In the simulation scenario of capacity versus 3D distance, we choose two carrier frequencies, namely 4.48 GHz and 78.11 GHz, in order to test the performance of InH indoor model in the cmWave and mmWave carrier along with the 3D distance.

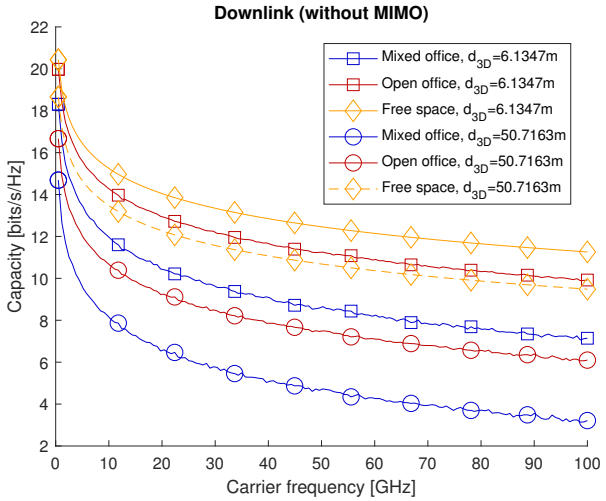

Fig. 2. Capacity versus the carrier frequency in both indoor mixed office and open office scenarios. The result is based on 1000 Monte Carlo runs.

The capacity results from Fig. 2 show that a high capacity above 18 bits/s/Hz, as targeted by some studies in Table III is achievable mostly at sub-GHz carrier frequencies. The more moderate target of 5 bits/s/Hz from Table III is achievable at all carrier frequencies up to 100 GHz for the open office InH model, but only at carrier frequencies below 50 GHz for mixed office InH model. We also notice from Fig. 2 that the open office InH model at small distances between the access node and the robot is only about 1 bit/s/Hz worse than the free space model.

In Fig. 3, likewise it indicates that the possibility of reaching 18 bits/s/Hz at high carrier frequency (i.e.,78.11GHz) does not exist, no matter under what scenarios. Discussing the capacity

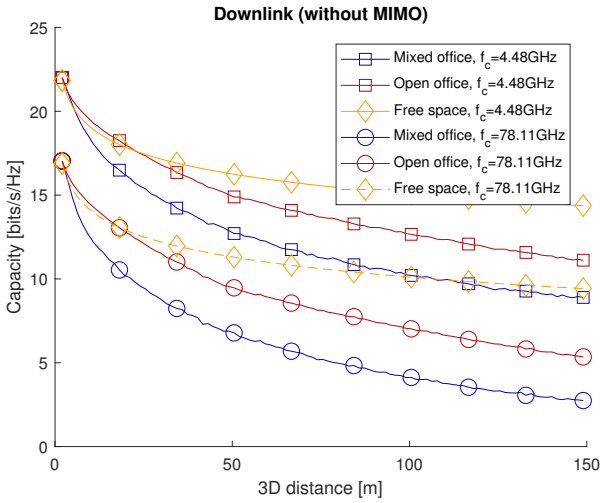

Fig. 3. Capacity versus the 3-D distance in both indoor mixed office and open office scenarios.The result is based on 1000 Monte Carlo runs.

from the angle of the 3D distance, we notice that high capacity could only be achieved in the near area for both the open office and mixed office InH models.

C. Outage probability

The rejection sampling method is applied as a numerical approach to compute the outage probability. The results of numerical approach are shown in Fig. 4. The figure is given along with the carrier frequency, and the total Monte Carlo runs are 100000 times. The sampling algorithm is given as below,

Algorithm 1 Outage probability of a specific carrier frequency

Require: shadowing ξ_{LOS} and ξ_{NLOS}, link budget from Table V, receiver sensitivity $P_{R_{min}}$ from Table IV, carrier frequency f_c, iterations R.

Draw $d_{3D}^{(i)} \sim \mathcal{U}(2, 150)$, set variable $count = 1$
for $i = 1 : R$ **do**
  Calculate path loss PL_{InH} according to eq. (5)
  if $PL_{InH} \geq P_T + G_T - L_T + G_R - L_R - P_{R_{min}}$ **then**
    $count = count + 1$
  else
    Continue to the next for loop
  end if
end for
Outage probability $p_{out} = \frac{count}{R}$

The theoretic analysis of outage probability is provided as well. In Section III, we mentioned that the path losses follow Gaussian distribution when only the shadowing is considered. The outage probability p_{out} is then equivalent to $1-\Phi(\frac{x-\mu_{PL}}{\sigma_{PL}})$, where $\Phi(\cdot)$ denotes the cumulative distribution function (CDF) of the standard normal distribution, $x = P_T + G_T - L_T + G_R - L_R - P_{R_{min}}$. The results of both theoretic and numerical analysis are shown in Figs. 4.

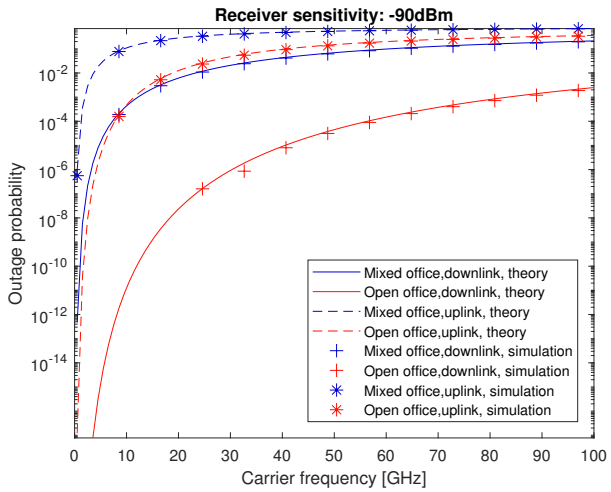

Fig. 4. Outage probability in -90 dBm sensitivity. In the simulation 100000 Monte Carlo runs are implemented.

one receiver sensitivity value applies in this simulation scenario, namely -90dBm (BLE case of Table IV). At a high receiver sensitivity (e.g., -146 dBm), we are able to reach very low or zero outage probabilities with both 3GPP InH channel models. At a lower receiver sensitivity (e.g., -90 dBm, the lowest receiver sensitivity in Table IV), the 10^{-2} outage probability target of Table III are achieved at sub-GHz carrier frequencies and frequencies below 3 GHz for both InH models and both in uplink and downlink, and they are achieved at carrier frequencies up to 100 GHz for the open-office InH model in downlink case.

Remark 1: We would like to mention that the difference of the results in the simulation and theory are mainly caused by the number of Monte Carlo runs. The results of simulation will eventually converge to the theoretic analysis, when the number of Monte Carlo runs tends to the infinity. However, the Monte Carlo method is very time-consuming, we could only push the result of simulation as close to the theoretic results as possible.

VII. Conclusions

This paper focused on the 3GPP indoor hotspot models (mixed office and open office) in the context of indoor industrial applications. We have compared the InH models between them and with the free space model and we have looked at the path losses, capacity, and outage probabilities achievable under these models. We have also compared the achievable figures with target values found in the literature and we have observed that the industrial targets can be reached under an open-office InH model at any carrier frequency, and under a mixed-office InH model at sub-GHz or few GHz carrier frequencies. For industrial applications in mm-waves bands (i.e., carrier frequencies above 30 GHz) more research studies are needed to improve the achievable capacity and outage probabilities.

Acknowledgement

The authors express their warm thanks to the Academy of Finland (project number 313039) for its financial support.

References

[1] S. A. Ashraf, I. Aktas, E. Eriksson, K. W. Helmersson, and J. Ansari, "Ultra-reliable and low-latency communication for wireless factory automation: From lte to 5g," in *2016 IEEE 21st International Conference on Emerging Technologies and Factory Automation (ETFA)*, pp. 1–8, Sept 2016.

[2] I. Aktas, M. H. Jafari, J. Ansari, T. Dudda, S. A. Ashraf, and J. C. S. Arenas, "Lte evolution - latency reduction and reliability enhancements for wireless industrial automation," in *2017 IEEE 28th Annual International Symposium on Personal, Indoor, and Mobile Radio Communications (PIMRC)*, pp. 1–7, Oct 2017.

[3] T. X. Quach, H. Tran, E. Uhlemann, and M. T. Truc, "Secrecy performance of cognitive cooperative industrial radio networks," in *2017 22nd IEEE International Conference on Emerging Technologies and Factory Automation (ETFA)*, pp. 1–8, Sept 2017.

[4] G.-T. S. G. R. A. Network, "Study on 3d channel model for lte (release 12)." 3GPP TR 36.873 V12.7.0 (2017-12), 2017.

[5] G.-T. S. G. R. A. Network, "Study on channel model for frequencies from 0.5 to 100 ghz." 3GPP TR 38.901 V14.3.0 (2017-12), 2017.

[6] Y. Li, Y. Liu, X. Zhang, and Q. Quan, "Dynamic channel model and performance analysis for lte-hi," in *2017 IEEE Wireless Communications and Networking Conference (WCNC)*, pp. 1–5, March 2017.

[7] T. S. Rappaport, S. Sun, and M. Shafi, "Investigation and comparison of 3gpp and nyusim channel models for 5g wireless communications," in *2017 IEEE 86th Vehicular Technology Conference (VTC-Fall)*, pp. 1–5, Sept 2017.

[8] B. Vejlgaard, M. Lauridsen, H. Nguyen, I. Z. Kovacs, P. Mogensen, and M. Sorensen, "Interference impact on coverage and capacity for low power wide area iot networks," in *2017 IEEE Wireless Communications and Networking Conference (WCNC)*, pp. 1–6, March 2017.

[9] Y. Ai, M. Cheffena, and Q. Li, "Radio frequency measurements and capacity analysis for industrial indoor environments," in *2015 9th European Conference on Antennas and Propagation (EuCAP)*, pp. 1–5, May 2015.

[10] L. R. Nair, B. T. Maharaj, and J. W. Wallace, "Capacity and robustness of single- and dual-polarized mimo systems in office and industrial indoor environments," in *IEEE GLOBECOM 2007 - IEEE Global Telecommunications Conference*, pp. 4522–4526, Nov 2007.

[11] Y. Gao, T. Yang, and B. Hu, "Improving the transmission reliability in smart factory through spatial diversity with arq," in *2016 IEEE/CIC International Conference on Communications in China (ICCC)*, pp. 1–5, July 2016.